Chemical–mineralogical characterization of historical bricks from Ferrara: an integrated bulk and micro-analytical approach

GIANLUCA BIANCHINI, ELENA MARROCCHINO, ALESSANDRO MORETTI & CARMELA VACCARO

Dipartimento di Scienze della Terra, Università degli Studi di Ferrara, Via Saragat 1, I-44100 Ferrara, Italy (e-mail: bncglc@unife.it)

Abstract: In this paper we present bulk X-ray fluorescence–X-ray diffraction (XRF/XRD) and microanalytical scanning electron microscope–electron microprobe analysis (SEM–EMPA) data on historical bricks from Medieval or Renaissance buildings of Ferrara (NE Italy) to provide insights into the nature and provenance of the raw material as well as clues on the sintering techniques. Chemical data indicate that the starting materials were obtained by mixing high Cr–Ni clay and subordinate sand (both quarried from the Po river alluvial deposits) with the possible introduction of a Na-rich flux component. Thin-section observation, XRD and micro-analytical data indicate the presence of key accessory phases such as pyroxene, amphibole, epidote and rare olivine in the pre-fired mineral assemblage, confirming the utilization of the Po river sediments. Recognition of neo-formation firing phases (e.g. melilite, wollastonite), together with composition of micas, amphiboles and interstitial glasses, indicate kiln temperatures between *c.* 800 and 1000 °C. This provides guidelines for making new compatible and durable bricks to be utilized for restoration, and contributes to the preservation of historical masonry.

Ancient bricks from Medieval and Renaissance buildings of Ferrara (NE Italy) have been studied using bulk techniques that analyse a few grams of homogenized (powdered) sample, and microanalytical techniques that allow composition analysis of single phases of materials that are heterogeneous at a micrometre scale.

This characterization provides useful clues to constrain the provenance of the original raw materials and the historical firing techniques. These data provide information useful to understand the physico-chemical behaviour of the studied bricks that will be helpful in future preservation and restoration strategies.

Historical background

The Medieval city of Ferrara (NE Italy, Fig. 1), is located in the eastern part of the Po alluvial plain, where at that time the Primaro river branched off from the main course of Po river (Bondesan *et al.* 1995; Ferri & Giovannini 2000). This geographical position, situated on a major waterway at a natural crossroads between the Adriatic Sea and the Po alluvial plain, contributed to the flourishing of the city, which peaked during the Renaissance. In this period, the Este family promoted a further fortification of the wall ring and embellished the city centre in a grandiose style with numerous sumptuous palaces. This building boom utilized bricks (cotto ferrarese) and mortars as the dominant building materials. The use of these construction materials is related to the geographical position and the geomorphological framework of the Ferrara area, which is characterized by the widespread presence of silico-clastic sediments (and the lack of rock outcrops; Amorosi *et al.* 2002).

Bricks and a few cotto decorative elements were collected from some important historical monuments of the city. These included the Monastery of Sant'Antonio in Polesine (built in several phases during the 12th–16th centuries), the Church of Santa Maria in Vado (founded in the 10th century and extensively modified in the 15th–16th centuries), the Church of Santo Stefano (founded in the 10th century, but rebuilt in the 15th–16th centuries), the Cathedral of Ferrara (apse, 15th–16th centuries), the Schifanoia Palace ('Hall of Stuccoes', 15th–16th centuries), and the surrounding city walls (15th century).

Bulk chemical composition of historical bricks from Ferrara

Chemical composition (major and trace elements) of terracottas sampled from the

From: MAGGETTI, M. & MESSIGA, B. (eds) 2006. *Geomaterials in Cultural Heritage*. Geological Society, London, Special Publications, **257**, 127–140.
0305-8719/06/$15.00

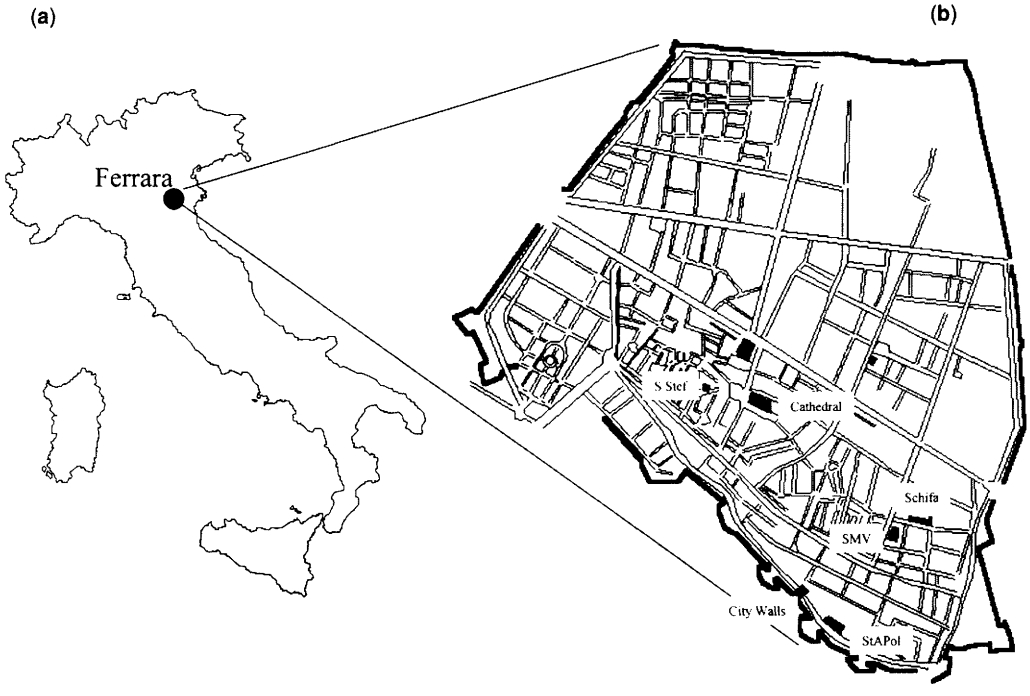

Fig. 1. Sketch map showing (**a**) the geographical position of Ferrara; (**b**) the locations of the studied historical buildings. S. Stef, Church of Santo Stefano; Schifa, Schifanoia Palace; SMV, Church of Santa Maria in Vado; StAPol, Monastery of Sant'Antonio in Polesine.

historical buildings of Ferrara and its city walls was determined by X-ray fluorescence (XRF) using a Philips PW1400 spectrometer. The method was calibrated with a wide range of natural standards, and the precision and accuracy were better than 5%. Representative analyses of bricks and cotto decorative elements from historical buildings and the city walls are presented in Table 1. Major element analyses have been recalculated and summed to 100% including LOI (loss of ignition at 1100 °C), and trace element data are expressed in parts per millions (ppm).

To investigate the nature of the raw material, these results were compared with data that included natural sediments from the Po alluvial plain around Ferrara (Bianchini *et al.* 2002*a*, plus our unpublished data; Table 2) and plotted using bivariate diagrams with SiO_2 wt% as a variation index (Fig. 2). The relatively restricted CaO range typical of the studied terracotta (in contrast to the high CaO variability recorded in the local clays) suggests that the most carbonate-rich pelitic sediments were preferentially quarried as raw materials for brick production. This means that the Ferrara brick-makers noticed that CaO-rich clays ultimately led to bricks characterized by better physico-mechanical properties (e.g. higher compressive strength, higher durability) because carbonates have a positive influence on brick textures by promoting a higher degree of vitrification (Elert *et al.* 2003).

The Al_2O_3 content of the studied bricks is generally lower (and the SiO_2 content slightly higher) than that of the local clays, showing a rough trend towards the composition of the local sands. The occurrence of coherent trends in other plots (see the K_2O v. SiO_2 diagram) indicates that such sands were used to temper the original clay body. This is confirmed by thin-section analysis, in which we observed that several samples are not homogeneous and are characterized by distinct textural domains (e.g. portions characterized by different grain sizes; presence of detrital grains). This suggests that the original raw materials were often mixed to obtain a suitable composition.

On the other hand, the excess of Na_2O recorded in the studied materials (compared with the local clay composition) cannot be ascribed to the introduction of sand in the starting body clay. This feature could be induced by

Table 1. *Major (wt%) and trace element (ppm) composition of bricks and terracotta samples from the historic buildings and city walls of Ferrara.*

	Sant' Antonio in Polesine Church (StAPol)							
	*	*	*	*	*	*	*	*
	EMT	19MT	32MTint	104MT	105MT	107MT	122MT	154MT
SiO_2	54.80	52.71	54.04	52.03	54.11	53.11	55.27	52.55
TiO_2	0.71	0.74	0.64	0.75	0.68	0.71	0.67	0.73
Al_2O_3	14.91	15.21	13.34	14.52	15.14	15.35	14.77	15.11
Fe_2O_3	5.78	6.48	5.32	6.16	5.79	6.22	5.76	6.56
MnO	0.12	0.12	0.15	0.14	0.11	0.12	0.11	0.13
MgO	4.79	5.17	3.51	4.20	5.06	5.26	4.90	4.86
CaO	10.28	10.97	13.66	13.80	9.94	10.21	9.42	13.14
Na_2O	1.91	1.57	1.48	0.97	1.95	1.65	1.90	1.20
K_2O	2.04	2.29	2.09	2.35	2.08	2.73	2.24	2.27
P_2O_5	0.20	0.19	0.23	0.18	0.20	0.23	0.18	0.18
LOI	4.46	4.55	6	4.90	4.95	4.43	4.80	3.27
Total	100	100	100	100	100	100	100	100
Ni	152	167	156	127	153	165	150	166
Co	21	20	21	18	21	21	19	21
Cr	239	252	202	169	231	222	221	241
V	89	127	114	116	110	118	98	121
	Cathedral							
	=	=	=	*	*	*	*	*
	C1	C8	C9	MT2	MT3	MT6	MT14	MT15
SiO_2	57.76	54.91	53.90	55.90	53.89	54.59	52.20	54.48
TiO_2	0.65	0.64	0.63	0.68	0.62	0.64	0.62	0.65
Al_2O_3	13.64	13.96	14.28	13.86	12.60	13.82	12.55	13.64
Fe_2O_3	5.44	5.50	5.53	5.76	5.20	5.40	5.15	5.50
MnO	0.11	0.12	0.11	0.12	0.10	0.10	0.11	0.11
MgO	4.14	4.18	4.22	4.69	4.42	4.05	4.25	4.07
CaO	9.22	9.13	9.02	11.49	11.67	8.48	11.33	10.22
Na_2O	1.47	1.28	1.12	1.51	1.48	1.08	1.52	1.40
K_2O	2.13	2.39	2.54	2.20	2.42	2.30	2.66	2.35
P_2O_5	0.25	0.27	0.21	0.25	0.26	0.21	0.28	0.25
LOI	5.2	7.63	8.45	3.54	7.34	9.32	9.32	7.33
Total	100	100	100	100	100	100	100	100
Ni	143	148	148	161	143	145	133	142
Co	17	14	19	21	14	17	17	17
Cr	201	187	194	216	229	188	199	201
V	92	104	102	100	133	112	98	102
	Santo Stefano Church (S.Stef)							
	=	=	*	=	=	=		
	SL36	SL37	SL39	SL40	SL41	SL46		
SiO_2	55.69	56.30	56.50	49.03	56.61	51.07		
TiO_2	0.72	0.67	0.72	0.68	0.71	0.67		
Al_2O_3	14.32	13.37	15.07	14.51	15.47	15.57		
Fe_2O_3	6.42	5.90	6.33	6.27	6.07	5.85		
MnO	0.13	0.12	0.12	0.11	0.12	0.08		
MgO	4.14	4.65	4.54	3.84	5.56	5.00		
CaO	10.96	12.36	8.47	10.81	10.29	9.40		
Na_2O	0.87	0.99	0.72	0.68	1.21	0.62		
K_2O	2.31	2.05	2.46	2.30	2.08	2.48		
P_2O_5	0.43	0.48	0.34	0.47	0.35	0.28		
LOI	4.02	3.11	4.73	11.31	1.52	8.97		
Total	100	100	100	100	100	100		
Ni	144	140	151	152	155	159		
Co	19	20	22	19	22	21		
Cr	252	239	233	218	242	304		
V	100	95	98	100	93	124		

(Continued)

Table 1. *Continued*

	City Walls									
	*	*	*	*	*	*	*	*	*	*
	1EG	7EG	9EG	17EG	19EG	22EG	33EG	35EG	37EG	40EG
SiO_2	54.70	53.37	52.06	53.03	54.87	53.36	51.73	47.80	51.11	53.54
TiO_2	0.74	0.70	0.76	0.73	0.79	0.69	0.64	0.69	0.73	0.70
Al_2O_3	16.16	14.47	16.80	15.94	16.78	14.92	13.95	14.96	15.80	15.26
Fe_2O_3	6.62	5.96	7.18	6.70	7.10	6.03	5.46	6.34	6.46	5.99
MnO	0.11	0.11	0.12	0.13	0.12	0.12	0.12	0.12	0.13	0.12
MgO	4.68	4.32	4.93	5.13	5.14	4.40	4.72	4.74	5.61	4.82
CaO	9.76	13.26	10.67	11.89	9.51	12.94	11.92	11.43	8.87	11.16
Na_2O	1.24	1.23	1.04	1.16	1.23	1.27	0.84	1.26	1.39	1.33
K_2O	2.48	2.09	2.66	2.38	2.55	2.24	2.59	2.52	2.50	2.22
P_2O_5	0.29	0.28	0.40	0.28	0.25	0.30	0.33	0.29	0.21	0.33
LOI	3.23	4.20	3.38	2.62	1.66	3.74	7.70	9.85	7.18	4.52
Total	100	100	100	100	100	100	100	100	100	100
Ni	179	159	199	197	195	157	144	166	185	165
Co	19	18	19	22	25	22	16	25	22	20
Cr	264	200	288	246	248	204	188	238	253	231
V	104	97	118	102	116	80	91	87	131	82

	Santa Maria in Vado Church (SMV)							
	*	*	*	*	=	*	*	=
	SL25	SL26	SL27	SL28	SL29	N4	N13	N20
SiO_2	56.50	53.54	53.10	50.78	54.58	54.46	50.58	49.28
TiO_2	0.70	0.74	0.68	0.65	0.70	0.72	0.67	0.60
Al_2O_3	16.08	16.95	14.30	14.92	15.46	16.34	14.66	12.78
Fe_2O_3	6.08	6.78	5.90	5.69	6.24	6.20	5.91	5.04
MnO	0.11	0.09	0.12	0.11	0.13	0.08	0.12	0.10
MgO	4.75	5.15	5.54	4.64	4.77	4.98	4.92	3.57
CaO	8.12	8.79	11.86	11.15	10.34	7.72	10.86	12.00
Na_2O	0.89	0.88	1.07	0.73	1.10	0.93	0.88	1.12
K_2O	2.47	2.72	2.02	2.63	2.14	2.76	2.48	2.06
P_2O_5	0.28	0.28	0.38	0.35	0.36	0.17	0.22	0.23
LOI	4.01	4.08	5.03	8.35	4.19	5.63	8.72	13.22
Total	100	100	100	100	100	100	100	100
Ni	148	187	156	150	160	164	159	112
Co	22	25	21	22	22	23	19	15
Cr	210	262	243	207	259	233	240	170
V	114	135	117	114	110	120	117	81

	Schifanoia Palace (Schifa)							
	*	*	*	*	*	*	*	*
	SE 15 P	SE 9 P	SE 19 P	SN 6 P	SE 20 P	SS 5 P	SS 4 P	SE 10 P
SiO_2	51.66	53.11	53.46	54.05	54.34	54.61	54.89	58.23
TiO_2	0.70	0.76	0.73	0.68	0.71	0.75	0.76	0.80
Al_2O_3	14.77	15.49	15.30	14.35	14.83	15.26	15.40	14.78
Fe_2O_3	6.08	6.69	6.37	6.04	6.06	6.50	6.61	6.89
MnO	0.13	0.13	0.12	0.13	0.12	0.13	0.13	0.14
MgO	4.87	4.71	5.17	5.00	4.88	5.28	5.31	3.56
CaO	11.80	11.46	11.87	10.94	11.01	10.19	11.24	10.88
Na_2O	1.16	1.34	1.33	1.53	1.56	1.61	1.36	1.47
K_2O	2.34	2.42	2.19	2.31	2.10	2.36	2.43	2.59
P_2O_5	0.17	0.21	0.20	0.20	0.19	0.19	0.19	0.28
LOI	6.31	3.68	3.28	4.77	4.20	3.12	1.7	0.38
Total	100	100	100	100	100	100	100	100
Ni	155	162	172	154	153	169	181	152
Co	22	23	21	20	19	22	24	20
Cr	227	243	250	224	229	251	262	221
V	112	123	92	103	112	120	107	111

Symbols: *, bricks; =, cotto decorative elements.

Labels: StAPol, bricks and terracotta elements from the Monastery of Sant'Antonio in Polesine; SMV, bricks and terracotta elements from the Church of Santa Maria in Vado; S.Stef, bricks and terracotta elements from the Church of Santo Stefano; Schifa, bricks and terracotta elements from Schifanoia Palace; Cathedral, bricks and terracotta elements from the Cathedral of Ferrara.

Table 2. *Major (wt%) and trace element (ppm) composition of natural sediments from the Ferrara surrounding*

	Low-Cr clay*				High-Cr clay*				Po river sands			
	SL8	SL9	SL10	SL14	SL4	SL16	SL17	SL18	ME1	F5C2	F6C4	F8C4
SiO_2	49.63	49.00	47.88	47.20	53.49	45.57	51.11	51.27	69.83	58.14	60.85	62.05
TiO_2	0.75	0.75	0.72	0.68	0.72	0.67	0.70	0.74	0.36	0.39	0.41	0.41
Al_2O_3	19.05	18.46	17.63	15.90	20.96	14.94	17.07	17.94	9.51	10.72	10.37	9.96
Fe_2O_3	6.95	7.09	6.49	6.76	6.06	6.09	6.14	6.51	2.66	3.52	3.64	3.34
MnO	0.10	0.12	0.10	0.14	0.04	0.12	0.07	0.07	0.07	0.06	0.08	0.08
MgO	3.15	3.03	3.01	2.99	3.20	4.32	4.69	4.23	3.85	4.23	3.47	3.31
CaO	6.47	7.65	7.93	9.72	1.32	11.04	6.37	4.82	6.10	10.31	8.79	9.03
Na_2O	0.35	0.36	0.39	0.48	0.71	0.53	0.67	0.48	1.98	1.53	1.79	1.79
K_2O	3.38	3.37	2.99	2.58	3.38	2.22	2.51	2.67	1.98	2.07	2.03	1.91
P_2O_5	0.18	0.24	0.24	0.28	0.00	0.33	0.17	0.15	0.08	0.11	0.12	0.12
LOI	9.98	9.95	12.62	13.27	10.14	14.16	10.5	11.12	3.58	8.91	8.46	8.00
Total	100	100	100	100	100	100	100	100	100	100	100	100
Ni	82	82	80	89	112	145	155	162	83	96	87	81
Co	20	20	18	18	17	21	29	32	13	14	12	10
Cr	136	143	134	122	268	210	288	281	138	132	138	124
V	163	155	148	144	174	124	146	158	40	59	56	55

*Analyses from Bianchini *et al.* (2002*a*).

soluble salts precipitated from Na-bearing aqueous solutions. However, the common occurrence of such Na_2O excess appears to be unrelated to the spatial distribution of the sampled bricks, some of which were located indoors and far from the floor (i.e. in a position not accessible to rain and/or ground water). Therefore, we suspect the addition of an 'exotic' Na-rich component as a fluxing agent incorporated during the firing phase. In this regard, excluding feldspar-rich lithologies (no enrichment in Al_2O_3 is observed) and salts such as Na_2CO_3 (not available in the area and too expensive in Medieval times), we speculate that either vegetable ash (obtained by burning seaweed?; see Chapman & Chapman 1980; Stiaffini 1999) or common marine salt (NaCl) were used. Introduction of the latter component would cause acceleration of mineral decomposition and subsequent crystallization of newly formed Ca-silicates. This would lower the prograde chemical reactions by *c.* 100–200 °C compared with those in NaCl-free ceramic systems (Maggetti & Von Der Crone 2004).

To address the provenance of the materials used, trace elements such as Ni and Cr (Fig. 3) indicate that the clay sediments around Ferrara can be separated into two groups characterized by high (Cr >180 ppm and Ni >100 ppm; High-Cr) and low (Cr <180 ppm and Ni <100 ppm; Low-Cr) contents. Bianchini *et al.* (2002*a*) showed that the Low-Cr sediments are characterized by a higher proportion of clay minerals in which smectite + mixed layers are more abundant than chlorite. The High-Cr sediments have a coarser grain size and a lower abundance of clay minerals, with chlorite (Mg-rich chlorite in this group of samples) predominating over smectite + mixed layers. Most of the studied Medieval or Renaissance bricks and terracotta elements seem to have been prepared starting from High-Cr sediments, as these clays show a chemical affinity with the present-day Po river sediments. The Low-Cr compositions (recorded in only a few samples) are analogous to the sediments of rivers flowing from the Bolognese Apennines. This probably means that Low-Cr clays were not available in the Ferrara area at that time. It is plausible to assume that Low-Cr clays were introduced in the area only after important hydraulic works in the 14th–16th centuries (Bondesan *et al.* 1995) resulted in the diversion of some Apenninic torrent-rivers (e.g. the Reno river) into the southern branches of the Po river (which was flowing south of Ferrara at that time).

The only two brick samples characterized by a Low-Cr affinity have to be considered as outliers, possibly representing 'allochthonous' bricks probably made in neighbouring areas where Reno river sediments were available.

Mineralogical composition of historical bricks from Ferrara

The mineralogical composition of the terracottas was investigated by X-ray powder diffraction (XRD) carried out using a Philips PW1860/00

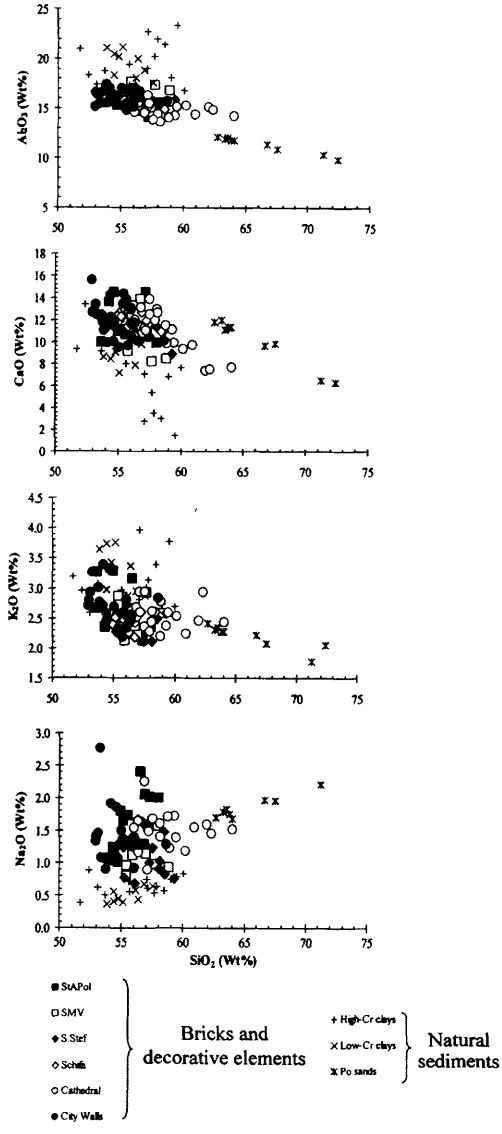

Fig. 2. Major element oxide bivariate diagrams. Analyses recalculated to 100% on an H_2O-CO_2 (LOI) free basis. Low-Cr clay, clays characterized by 'Apennine' affinity; High-Cr clays, clays closely comparable with the present-day fine sediments of the Po river; other abbreviations as in Figure 1.

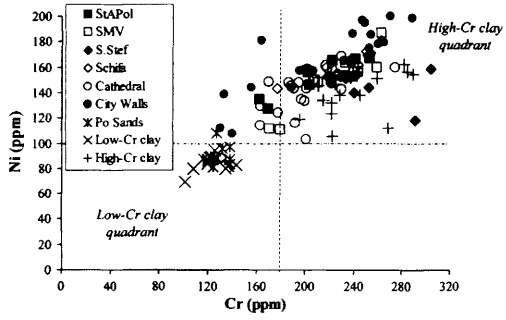

Fig. 3. Binary diagram for Ni v. Cr. Symbols and labels as in Figure 2. Quadrants delimited by dotted lines are useful to identify the nature of the clay raw materials (High-Cr v. Low-Cr).

diffractometer with graphite-filtered Cu-Kα radiation ($\lambda = 1.54$ Å). The diffraction patterns were collected in the 2θ angular range from 5 to 50°, with 5 seconds per step (0.02° 2θ). Most samples can be attributed to two distinct mineral parageneses (Bianchini *et al.* 2002*b*), as follows.

(1) Carbonate-bearing mineral assemblages (calcite ± dolomite) with ubiquitous quartz, illite/muscovite, biotite, iron oxides, alkaline feldspar and plagioclase. Amphibole has been detected, but it is not ubiquitous. Melilite ± wollastonite may also be present. These mineral associations have been recognized in samples from the Monastery of Sant'Antonio in Polesine, the Church of Santa Maria in Vado, and the city walls.

(2) Clinopyroxene-bearing (carbonate-free) mineral assemblages, with quartz, alkaline feldspar, plagioclase, iron oxides, melilite and wollastonite. Biotite and illite/muscovite are not ubiquitous and amphibole is rare. These mineral associations are typical for samples from the Church of Santo Stefano.

Both mineral parageneses can be observed in the samples from the Ferrara Cathedral, and mineral analyses are not yet available for Schifanoia samples.

These mineral parageneses do not appear to be consistent with the $(CaO + MgO)-Al_2O_3-SiO_2$ phase diagram (Fig. 4) in which the stability fields of firing phases are reported (Duminuco *et al.* 1998; Riccardi *et al.* 1999; Artioli *et al.* 2000). In Figure 4 the historical terracottas and the local clay composition plot mainly in the subtriangle Qz–Wo(Di)–An that corresponds to the quartz–wollastonite (diopside)–plagioclase equilibrium paragenesis. However, the common presence of carbonates and/or melilite (recorded by XRD in several samples) suggests that equilibrium conditions were not attained. This can be ascribed to the inhomogeneity of the original starting material, which consists of several micro-domains of different composition, and indicates a limited mobility of the chemical species during the firing processes (Duminuco *et al.* 1998; Riccardi *et al.* 1999).

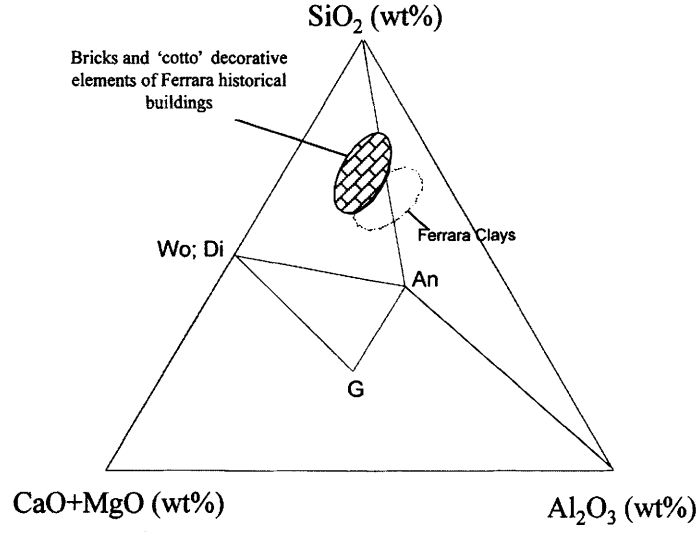

Fig. 4. $(CaO + MgO)-Al_2O_3-SiO_2$ phase diagram with compositions of historical bricks and terracotta elements from Ferrara. Compositions of firing phases, such as wollastonite, diopside, melilite (gehlenite) and plagioclase (anorthite), as well as relative tie-lines, are reported.

For the same reason, XRD bulk analyses cannot be considered completely reliable for the estimation of firing temperatures (Duminuco *et al.* 1998; Riccardi *et al.* 1999). This is evident when we consider some samples apparently characterized by 'misleading parageneses' containing carbonate minerals (an indicator of low firing temperature, i.e. <850 °C) and clinopyroxene and/or plagioclase (usually considered high-temperature products, i.e. >950 °C).

Microanalysis of constituent phases

The apparent incongruence in the recorded mineral parageneses can be examined using petrographic thin-section observation and *in situ* analytical techniques capable of investigating the reactions occurring in the various micro-domains. Microanalytical data have been obtained by: (1) scanning electron microscope (SEM) at the University of Ferrara using a Cambridge Stereoscan S-360 that provided semiquantitative analyses and sample images at a scale of a few tens of micrometres; (2) electron microprobe analysis (EMPA) using a CAMECA SX-50 at the CNR-IGG Institute of Padova with natural silicates and oxides as standards to provide quantitative analyses of the constituent phases.

Microprobe analyses were focused on coarse detritic grains possibly representing traces of the sand fraction introduced as temper. Among the mineral phases that constitute the sand we ignored common felsic minerals (i.e. quartz and feldspars) and focused investigation on accessory minerals, which provide more reliable insights into the raw material provenance as well as clues to the firing temperatures. In particular, micas (biotite and muscovite; Table 3) and amphiboles (Table 4) were examined and compared with data on their firing behaviour (i.e. temperature stability fields; Maggetti *et al.* 1984; Capel *et al.* 1985; Brindley & Lemaitre 1987; Dumunico *et al.* 1998; Riccardi *et al.* 1999; Cultrone *et al.* 2000; Bianchini *et al.* 2002*b*).

The K-poor composition of biotites (Table 3) does not reflect a mineral destabilization that occurs during the firing process. Similar compositions are commonly observed in a wide variety of sedimentary environments where pristine biotite crystals progressively release potassium, ultimately leading to the formation of hydrobiotite (Blum & Erel 1997; Murphy *et al.* 1998).

In sample MT3 muscovite is colourless, whereas hydrobiotite is nearly opaque but still homogeneous in composition, and amphibole is characterized by a wide compositional range, which includes coarse and homogeneous crystals of orange hornblende and edenite and brown pargasite. Actinolite microcrystals have been found within the finer matrix.

The orange colour of hornblende suggests oxidizing conditions and firing temperatures around 800 °C, and the absence of destabilization

Table 3. *Representative compositions of mica (muscovite and hydrobiotite) in historical bricks from Ferrara*

Sample:	MT3						MT15								
Mineral:	Muscovite		Hydrobiotite				Muscovite				Hydrobiotite			Destabilization products on hydrobiotite	
	MT3p3c	MT3p3d	MT3p4c	MT3p4d	MT3p4f	MT3p1d	MT15 2a	MT15 2b	MT15 3a	MT15 3a*	MT15 1b	MT15 2 h	MT15 2l	MT15 4a	MT15 4c
SiO_2	53.23	48.51	29.36	28.70	27.62	26.30	46.58	47.71	50.23	47.75	32.10	28.66	27.95	59.52	84.99
TiO_2	0.08	0.10	0.04	0.03	0.04	0.02	0.11	0.08	0.06	0.39	0.01	0.96	0.52	0.43	0.05
Al_2O_3	27.53	32.09	19.48	19.00	22.87	21.36	38.05	38.86	30.21	36.88	21.60	22.41	22.13	15.21	7.12
Cr_2O_3	0.00	0.04	0.05	0.05	0.02	0.03	0.00	0.00	0.00	0.04	0.00	0.01	0.05	0.06	0.00
FeO	3.48	1.93	28.11	28.33	27.62	30.31	0.33	0.34	1.25	0.86	22.71	24.12	24.56	9.98	1.04
MnO	0.01	0.00	0.05	0.08	0.14	0.28	0.07	0.02	0.09	0.00	0.29	0.02	0.04	0.10	0.07
MgO	3.22	1.95	15.40	16.40	15.96	10.53	0.26	0.20	2.71	0.53	12.22	13.52	12.75	3.66	0.67
CaO	0.10	0.11	0.22	0.38	0.03	0.97	0.32	0.18	0.81	0.03	0.37	0.32	0.42	0.06	0.03
Na_2O	1.41	0.85	0.97	0.87	0.66	1.05	1.90	1.18	2.91	0.98	1.96	1.93	2.18	1.59	1.05
K_2O	8.68	8.57	1.81	1.80	1.18	2.27	10.46	10.55	6.27	10.06	4.02	3.41	3.47	5.95	4.31
Total	97.73	94.14	95.48	95.64	96.14	93.13	98.09	99.13	94.54	97.53	95.27	95.37	94.08	96.55	99.32
Cations/11 oxygens															
Si	3.44	3.23	2.27	2.23	2.11	2.14	3.01	3.04	3.31	3.09	2.43	2.20	2.19	Non-stoichiometric	
Ti	0.00	0.01	0.00	0.00	0.00	0.00	0.01	0.00	0.00	0.02	0.00	0.06	0.03		
Al	2.10	2.52	1.78	1.74	2.06	2.05	2.90	2.91	2.35	2.81	1.93	2.03	2.05		
Cr	0.00	0.00	0.00	0.00	0.00	0.00	0.00	0.00	0.00	0.00	0.00	0.00	0.00		
Fe	0.19	0.10	1.82	1.84	1.76	2.06	0.02	0.02	0.07	0.05	1.44	1.55	1.61		
Mn	0.00	0.00	0.00	0.01	0.01	0.02	0.00	0.00	0.01	0.00	0.02	0.00	0.00		
Mg	0.31	0.19	1.78	1.90	1.81	1.28	0.03	0.02	0.27	0.05	1.38	1.55	1.49		
Ca	0.01	0.01	0.02	0.03	0.00	0.09	0.02	0.01	0.06	0.00	0.03	0.03	0.04		
Na	0.18	0.11	0.15	0.13	0.10	0.17	0.24	0.15	0.37	0.12	0.29	0.29	0.33		
K	0.72	0.73	0.18	0.18	0.12	0.24	0.86	0.86	0.53	0.83	0.48	0.33	0.35		
Total	6.95	6.88	8.00	8.05	7.97	8.04	7.08	7.01	6.96	6.97	7.99	8.04	8.09		

Atomic formula units (a.f.u.) on the basis of 11 oxygens.

Table 4. *Representative compositions of amphibole in historical bricks from Ferrara*

Sample:	MT3								C1	Experimental trial actinolite (fired at 800 °C)
Mineral:	Actinolite		Hornblende		Pargasite		Edenite		Actinolite	
	MT3p1e	MT3p1f	MT3p3a	MT3p3b	MT3p2c	MT3p2d	MT3p1b	MT3p1c	clc	
SiO_2	58.56	57.01	48.52	47.73	43.02	43.20	48.72	47.79	57.90	56.03
TiO_2	0.00	0.03	0.23	0.20	1.36	1.33	0.10	0.15	0.01	0.00
Al_2O_3	0.08	0.14	9.70	9.59	11.84	11.79	8.22	10.08	1.12	2.75
Cr_2O_3	0.00	0.06	0.09	0.20	0.07	0.04	0.00	0.00	0.11	0.29
FeO	3.78	3.46	11.85	11.83	15.06	15.27	13.81	14.81	5.85	5.94
MnO	0.10	0.10	0.19	0.30	0.18	0.20	0.34	0.39	0.22	0.15
MgO	22.20	21.58	13.86	13.75	10.35	9.94	12.74	11.95	20.83	19.69
CaO	13.33	13.57	12.79	12.55	11.82	11.50	9.92	9.49	12.01	12.27
Na_2O	0.21	0.11	0.98	1.03	1.30	1.42	2.45	2.53	0.65	0.95
K_2O	0.03	0.04	0.30	0.31	1.57	1.57	0.28	0.29	0.52	0.03
Total	98.30	96.11	98.50	97.51	96.58	96.26	96.57	97.47	99.20	98.11
Cations/24 oxygens										
Si	7.59	7.99	6.97	6.95	6.50	6.56	7.18	7.00	7.45	7.79
Ti	0.00	0.00	0.03	0.02	0.16	0.15	0.01	0.02	0.01	0.00
Al	0.01	0.02	1.64	1.65	2.11	2.11	1.43	1.74	1.09	0.45
Fe	0.41	0.41	1.42	1.44	1.90	1.91	1.70	1.82	0.69	0.69
Mn	0.01	0.01	0.02	0.04	0.02	0.03	0.04	0.05	0.02	0.02
Mg	4.28	4.51	2.97	2.98	2.33	2.25	2.80	2.61	3.60	4.08
Ca	3.08	2.04	1.97	1.96	1.92	1.87	1.57	1.49	1.97	1.83
Na	0.05	0.03	0.27	0.29	0.38	0.42	0.70	0.72	0.27	0.26
K	0.01	0.01	0.06	0.06	0.30	0.30	0.05	0.05	0.13	0.01
Total	15.44	15.02	15.35	15.38	15.63	15.60	15.48	15.50	15.21	15.12

Atomic formula units on the basis of 24 oxygens. Amphibole nomenclature according to Leake *et al.* (1997).

evidence indicates a temperature lower than 900 °C (Maggetti *et al.* 1984). Moreover, the persistence of actinolite (well equilibrated up to 800 °C in our firing experiments of the local clays, but not recorded at 900 °C; Fig. 5) would confirm that sample MT3 has been fired at a temperature between 800 and 900 °C.

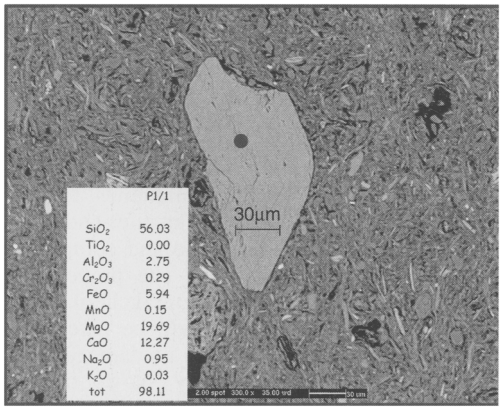

Fig. 5. Scanning electron micrograph of an actinolite amphibole in an experimental trial obtained by firing a local clay at 800 °C. Chemical analysis of the same crystal by EMPA is also reported.

The interpretation of the observed anhedral crystals of epidote (approaching the ideal $Ca_2(Fe,Al)_3(SiO_4)_3(OH)$ composition; Table 5) is not straightforward. This mineral is not reported as a common firing phase in ceramics. Its stability field appears to be confined at temperatures lower than 550 °C, as suggested by natural analogues in contact metamorphic parageneses (albite + epidote hornfels facies; Lentz *et al.* 1995; Moor & Gunderson 1995; Singoyi & Zaw 2001; Martínez-Serrano 2002). Therefore the observed epidote microcrystals may represent relicts of coarser crystals present in pre-fired mineral assemblages. This agrees with the presence of epidote in the sand fraction of sediments from the Po river (Marchesini *et al.* 2000).

In sample MT15 amphibole and epidote are not detected, muscovite is still colourless and hydrobiotite is totally destabilized. Microprobe investigation of hydrobiotite crystals indicates that they are not homogeneous and stoichiometric balanced compositions of hydrobiotite coexist with non-stoichiometric SiO_2–Al_2O_3–K_2O-rich

Table 5. *Representative compositions of epidote in historical bricks from Ferrara*

Sample:	C1	C1 epidote	C1	MT3 epidote
Mineral:	C1a	c1d	c1g	MT3p4e
SiO_2	38.06	38.94	39.31	37.40
TiO_2	0.06	0.14	0.08	0.01
Al_2O_3	22.41	28.08	28.28	21.04
FeO	13.00	5.25	5.60	13.55
MnO	0.09	0.06	0.15	0.19
MgO	0.07	0.06	0.07	0.00
CaO	23.93	24.58	24.58	22.68
Na_2O	0.05	0.04	0.03	0.00
K_2O	0.01	0.05	0.04	0.00
Total	97.68	97.20	98.13	94.87
Cations/25 oxygens				
Si	6.24	6.14	6.14	6.33
Ti	0.01	0.02	0.01	0.00
Al	4.33	5.22	5.21	4.20
Cr	0.00	0.00	0.00	0.00
Fe	1.78	0.69	0.73	1.92
Mn	0.01	0.01	0.02	0.03
Mg	0.02	0.01	0.02	0.00
Ca	4.20	4.15	4.12	4.11
Total	16.59	16.24	16.24	16.58

Atomic formula units on the basis of 25 oxygens.

compositions (Table 3). This sample is also characterized by the widespread presence of glassy films within the fine matrix that suggest a higher firing temperature compared with sample MT3 (probably approaching 1000 °C).

The persistence of carbonate cannot be used as an indicator of low firing temperature because the reactivity of large crystals of carbonate (possibly introduced as temper) is often limited to surfaces and would allow carbonate preservation as a metastable phase at a higher temperature than expected. Moreover, experiments show that not all CaO could combine with other oxides to form new calc-silicate phases during firing. This would lead to rehydration of the free CaO and the formation of secondary calcite (Maggetti *et al.* 1984). Furthermore, carbonate could also be related to weathering processes that form 'secondary' calcite in microcracks and pores (Lopez-Arce & Garcia-Guinea 2005).

Clinopyroxene and plagioclase cannot be considered as indicators of high firing temperature because they occur as accessory minerals in natural sediments of the Ferrara surroundings (Marchesini *et al.* 2000) and could have been present in the pre-fired mineral assemblage. The observation of crystal habits (euhedral v. anhedral) is useful to discriminate between phases originally present in the pre-fired mineral assemblage and neoformed phases (Fig. 6).

Within the fine matrix of sample MT15, SEM analysis recorded extremely variable compositions (in terms of Si, Ca, Al and Mg; Figs 7 and 8). These analyses do not fit stoichiometrically with potential firing phases (e.g. wollastonite, melilite, clinopyroxene) and could be interpreted as the compositions of glassy blebs. The different glass compositions within the same sample may be related to lack of equilibrium melting, and result in the coexistence of different micro-domains that were not homogenized during the firing processes. This implies that during the incipient partial melting, the composition of the neoformed melt phase (glass) is strongly influenced by the particular paragenesis of each micro-domain.

Microanalysis also revealed, in sample MT15, the presence of euhedral crystals of olivine (Fig. 9). This may represent evidence for the origin of the raw materials. The persistence of olivine (a mineral very susceptible to weathering processes) in the mineral assemblage of the starting sediments, together with the high Ni–Cr clay content, suggests that sediments from the Po (a river hydrological basin that contains mafic and ultramafic rocks) may be the source. This hypothesis is strengthened by the presence of olivine (Fig. 10) in experimental brick trials manufactured in our laboratories using alluvial clays of the Po river.

Conclusions

In this paper, chemical and mineralogical characterization of bricks and terracotta elements from historical buildings and city walls of Ferrara has allowed us to evaluate the nature of the original raw material (i.e. clay-rich sediment of local provenance) and to define technological information regarding the manufacture (i.e. firing temperatures between *c.* 800 and 1000 °C). This information provides guidelines for the production and use of new bricks, tiles and terracotta elements that are durable and compatible with the historical materials. The proper preservation of ancient architectural heritage is extremely important and should be taken into account during the restoration of damaged historical masonries. This study shows that to characterize the old materials and to establish the causes of the decay, as well as to plan for suitable protective or restoration treatment, it is necessary to identify and characterize the materials that were used to make these

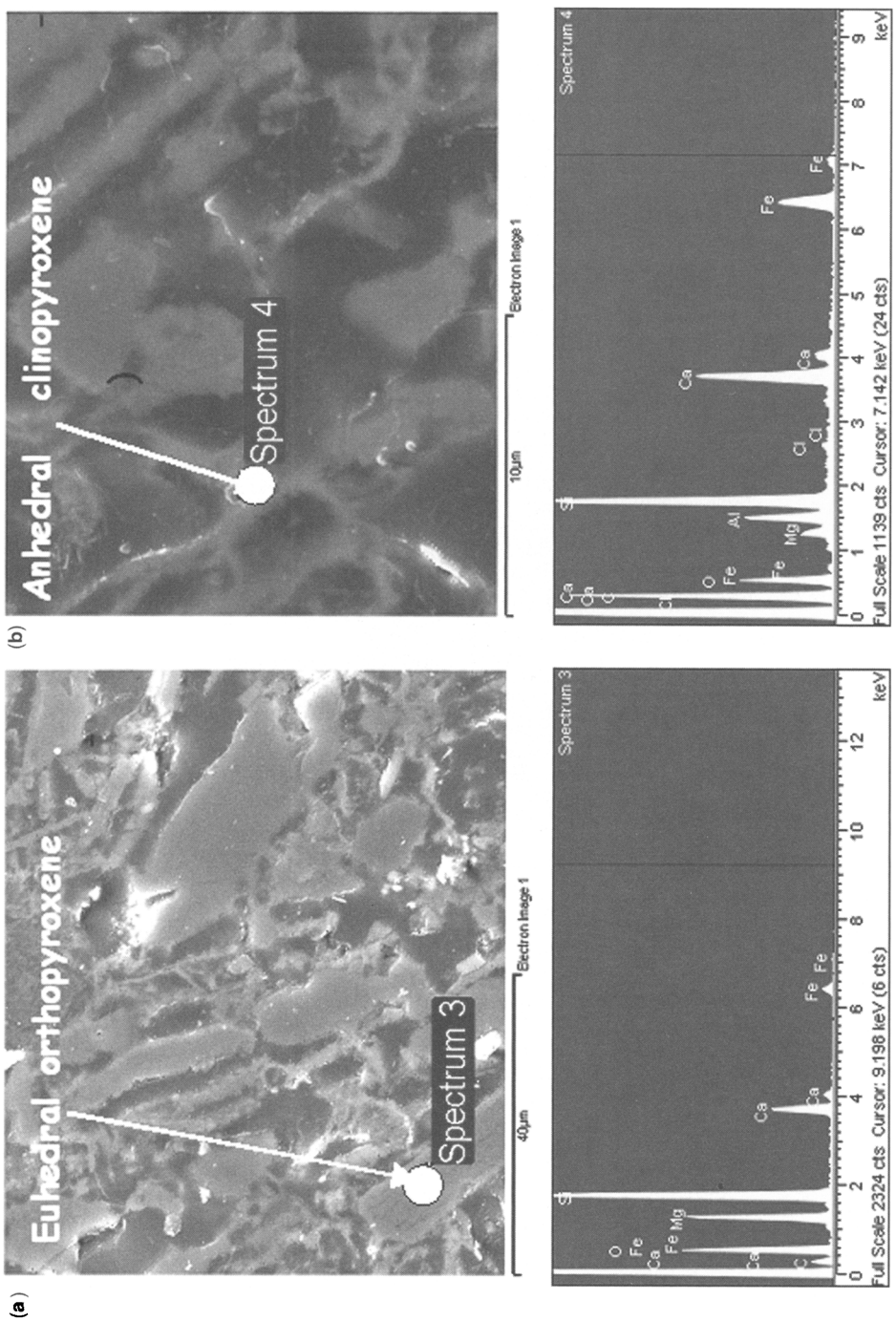

Fig. 6. Scanning electron micrographs (and EDS spectra) of pyroxene crystals recorded in sample MT15; (**a**) euhedral orthopyroxene plausibly present in the pre-firing mineral assemblage; (**b**) anhedral clinopyroxene microcrystal in the matrix (plausible neoformation).

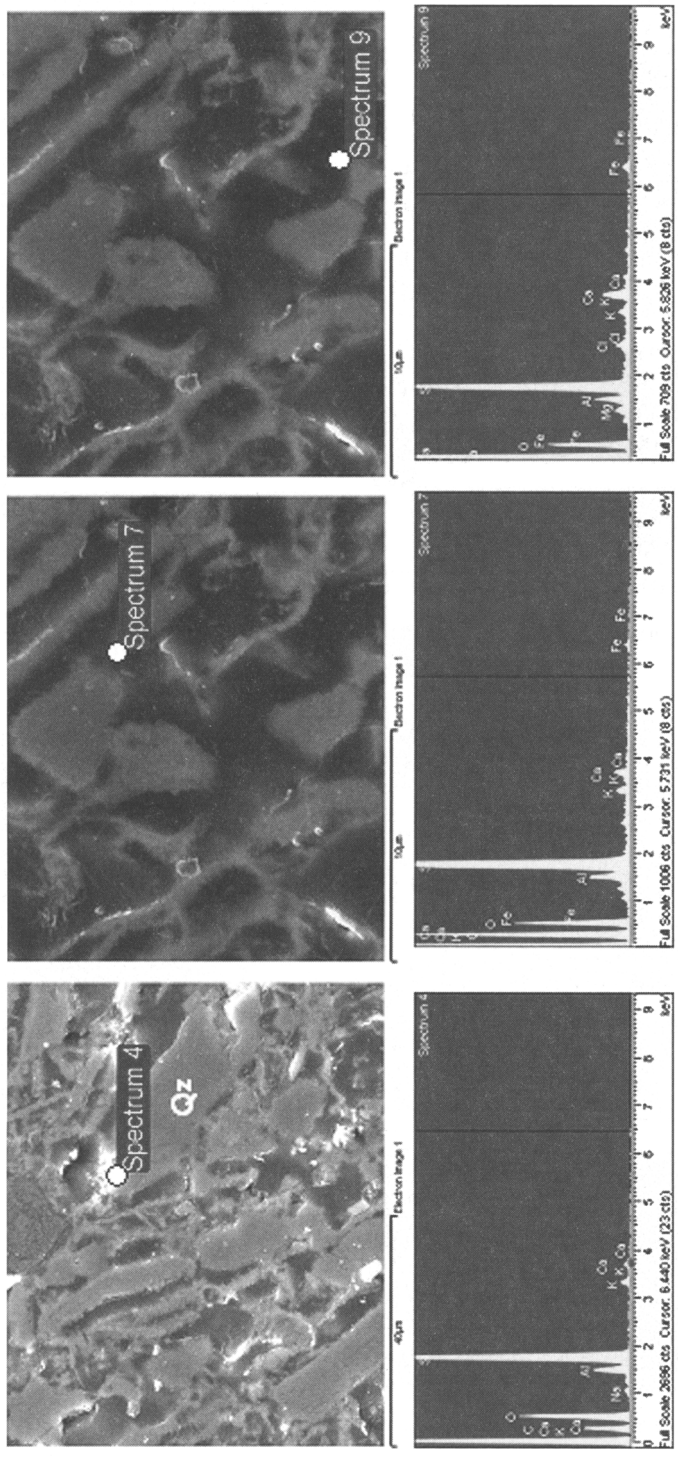

Fig. 7. Scanning electron micrographs (and EDS spectra) of silica-rich glassy patches within the matrix of sample MT15.

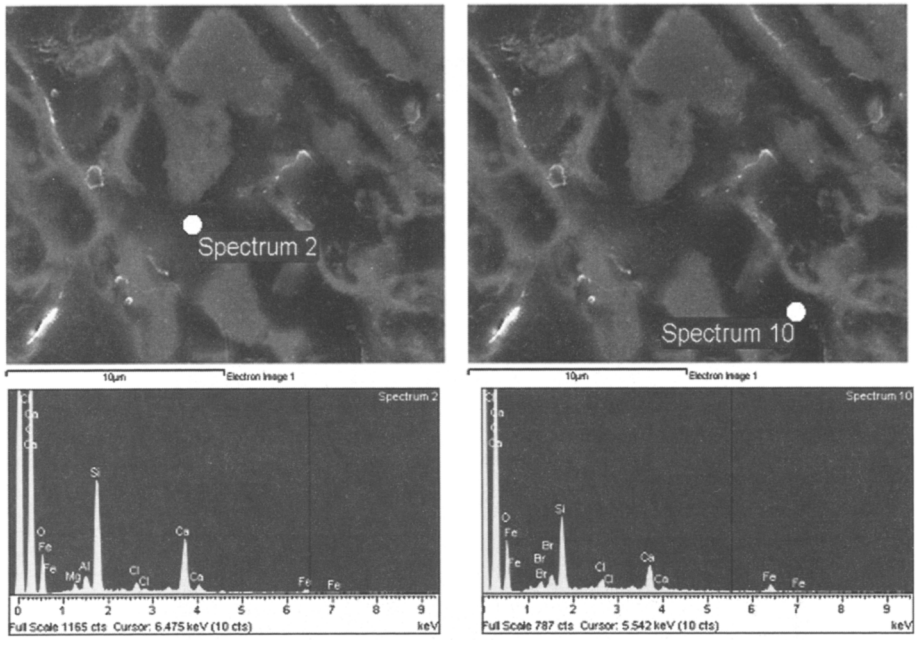

Fig. 8. Scanning electron micrographs (and EDS spectra) of calcium-rich glassy patches within the matrix of sample MT15.

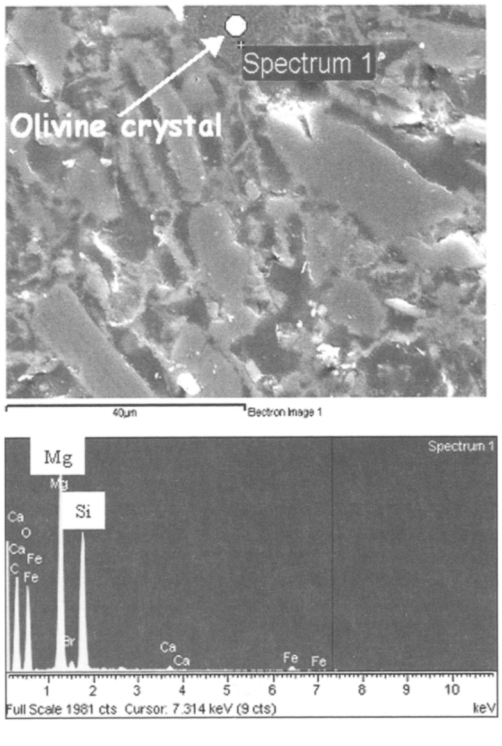

Fig. 9. Scanning electron micrographs (and EDS spectrum) of a euhedral olivine crystal in sample MT15.

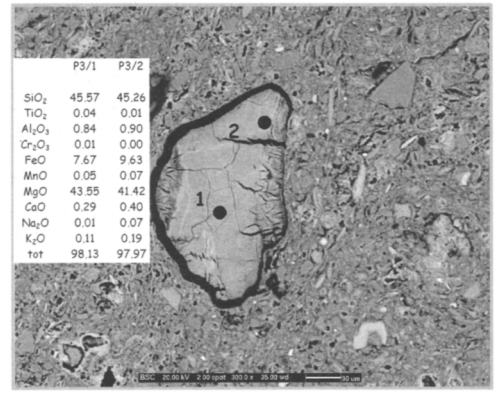

Fig. 10. Scanning electron micrographs of an olivine crystal in an experimental trial obtained by firing a local clay at 800 °C. Chemical analyses of the same crystal by EMPA are also reported.

architectural elements. This gives the restorer adequate information for choosing suitable new materials when replacement is necessary and to avoid incorrect restoration materials, such as were used in the Piazza Municipale of Ferrara, where new floor tiles were totally damaged and broken by freeze–thaw cycles during the first winter.

L. Beccaluva and F. Siena are kindly acknowledged for their preliminary review of the manuscript. The authors are also grateful to R. Tassinari (Università di Ferrara) and R. Carampin (CNR-IGG, Padova) for their analytical assistance, and to the reviewers for their constructive comments.

References

AMOROSI, A., CENTINEO, M. C., DINELLI, E., LUCCHINI, F. & TATEO, F. 2002. Geochemical and mineralogical variations as indicators of provenance changes in Late Quaternary deposits of SE Po Plain. *Sedimentary Geology*, **151**, 273–292.

ARTIOLI, G., BAGNASCO GIANNI, G., BRUNI, S., CARIATI, F., FERMO, P., MORIN, S. & RUSSO, U. 2000. Studio spettroscopico della tecnologia di cottura di ceramiche etrusche dagli scavi di Tarquinia. *In*: *Atti del I Congresso di Archeometria*. Patron Editore, Bologna, 335–349.

BIANCHINI, G., LAVIANO, R., LOVO, S. & VACCARO, C. 2002*a*. Chemical–mineralogical characterization of clay sediments around Ferrara (Italy): a tool for an environmental analysis. *Applied Clay Science*, **21**, 165–176.

BIANCHINI, G., MARTUCCI, A. &VACCARO, C. 2002*b*. Petro-archaeometric characterization of 'cotto ferrarese': bricks and terracotta elements from historic buildings of Ferrara. *Periodico di Mineralogia*, **71**, 101–111.

BLUM, J. D. & EREL, Y. 1997. Rb–Sr isotope systematics of a granitic soil chronosequence: the importance of biotite weathering. *Geochimica et Cosmochimica Acta*, **61**, 3193–3204.

BONDESAN, M., FERRI, R. & STEFANI, M. 1995. Rapporti fra lo sviluppo urbano di Ferrara e l'evoluzione idrografica, sedimentaria e geomorfologica del territorio in Ferrara nel Medioevo. *In*: *Topografia storica e archeologia urbana*. Casalecchio di Reno, Bologna, 27–42.

BRINDLEY, G. & LEMAITRE, J. 1987. Thermal, oxidation and reduction reactions of clay minerals. *In*: NEWMAN, A. C. D. (ed.) *Chemistry of Clays and Clay Minerals. Mineralogical Society, London*, Monograph, **6**, 319–370.

CAPEL, J., HUERTAS, F. & LINARES, J. 1985. High temperature reactions and use of Bronze Age pottery from La Mancha, Central Spain. *Mineralogica et Petrographica Acta*, **29-A**, 563–575.

CHAPMAN, V. J. & CHAPMAN, D. S. 1980. *Seaweeds and their Uses*. Chapman and Hall, London.

CULTRONE, G., SEBASTIAN-PARDO, E., CAZALLA, O., RODRIGUEZ-NAVARRO, C. & DE LA TORRE, M. J. 2000. Mineralogical changes during brick production in laboratory experiments. *In*: *Quarry–Laboratory–Monument International Congress, Pavia 2000, Proceedings Volume 1*, 253–258.

DUMINUCO, P., MESSIGA, B. & RICCARDI, M.P. 1998. Firing processes of natural clays. Some microtextures and related phase compositions. *Thermochimica acta*, **321**, 185–190.

ELERT, K., COLTRONE, G., NAVARRO, C. R. & PARDO, E. S. 2003. Durability of bricks used in the conservation of historic buildings—influence of composition and microstructure. *Journal of Cultural Heritage*, **4**(2) 91–99.

FERRI, R. & GIOVANNINI, A. 2000. Analisi dello sviluppo urbanistico della città di Ferrara nel quadro dell'evoluzione geomorfologica del territorio circostante. *In*: GALLINA, M. (ed.) *Dal Suburbium al Faubourg: evoluzione di una realtà urbana*. ET, Milan, 9–24.

LEAKE, B. E., WOOLLEY, A. R., ARPS, C. E. S., *et al.* 1997. Nomenclature of amphiboles: Report of the Subcommittee on Amphiboles of the International Mineralogical Association, Commission on New Minerals and Mineral Names. *Mineralogical Magazine*, **61**, 295–321.

LENTZ, D. R., WALKER, J. A. & STIRLING, J. A. R. 1995. Millstream Cu–Fe skarn deposit: an example of a Cu-bearing magnetite-rich skarn system in northern New Brunswick. *Exploration and Mining Geology*, **4**, 15–31.

LOPEZ-ARCE, P. & GARCIA-GUINEA, J. 2005. Weathering traces in ancient bricks from historic buildings. *Building and Environment*, **40**, 929–941.

MAGGETTI, M. & VON DER CRONE, M. 2004. Mineral reactions in synthetic clay NaCl system. *Abstracts from the 32nd International Geological Congress, Florence, 2004; Session T16.01—Geoarcheometry: geomaterials in cultural heritage*.

MAGGETTI, M., WESTLEY, H. & OLIN, J. S. 1984. Provenance and technical studies of Mexican majolica using elemental and phase analysis. *In*: LAMBERT, J. B. (ed.) *Archaeological Chemistry III. American Chemical Society*, Advances in Chemistry Series, **205**, 151–191.

MARCHESINI, L., AMOROSI, A., CIBIN, U., ZUFFA, G., SPADAFORA, E. & PRETI, D. 2000. Sand composition and sedimentary evolution of a Late Quaternary depositional sequence, Northwestern Adriatic coast, Italy. *Journal of Sedimentary Research*, **70**, 829–838.

MARTÍNEZ-SERRANO, R. G. 2002. Chemical variations in hydrothermal minerals of the Los Humeros geothermal system, Mexico. *Geothermics*, **31**, 579–612.

MOOR, J. N. & GUNDERSON, R. P. 1995. Fluid inclusion and isotopic systematics of an evolving magmatic-hydrothermal system. *Geochimica et Cosmochimica Acta*, **59**, 3887–3907.

MURPHY, S. F., BRANTLEY, S. L., BLUM, A. E., WHITE, A. F. & DONG, H. 1998. Chemical weathering in a tropical watershed, Luquillo Mountains, Puerto Rico: II. Rate and mechanism of biotite weathering. *Geochimica et Cosmochimica Acta*, **62**, 227–243.

RICCARDI, M. P., MESSIGA, B. & DUMINUCO, P. 1999. An approach to the dynamics of clay firing. *Applied Clay Science*, **15**, 393–409.

SINGOYI, B. & ZAW, K. 2001. A petrological and fluid inclusion study of magnetite–scheelite skarn mineralization at Kara, Northwestern Tasmania: implications for ore genesis. *Chemical Geology*, **173**, 239–253.

STIAFFINI, D. 1999. *Il vetro nel Medioevo*. Fratelli Palombi, Rome.